Spin-gap study of the spin-$\frac{1}{2}$ J_1–J_2 model on the triangular lattice

R. F. Bishop and P. H. Y. Li

School of Physics and Astronomy, Schuster Building, The University of Manchester, Manchester, M13 9PL, UK

PACS 75.10.Jm – Quantised spin models, including quantum spin frustration
PACS 75.10.Kt – Quantum spin liquids, valence bond phases and related phenomena

Abstract – We use the coupled cluster method implemented at high orders of approximation to study the spin-$\frac{1}{2}$ J_1–J_2 model on the triangular lattice with Heisenberg interactions between nearest-neighbour and next-nearest-neighbour pairs of spins, with coupling strengths $J_1 > 0$ and $J_2 \equiv \kappa J_1 > 0$, respectively. In the window $0 \leq \kappa \leq 1$ we find that the 3-sublattice 120° Néel-ordered and 2-sublattice 180° stripe-ordered antiferromagnetic states form the stable ground-state phases in the regions $\kappa < \kappa_1^c = 0.060(10)$ and $\kappa > \kappa_2^c = 0.165(5)$, respectively. The spin-triplet gap is found to vanish over essentially the entire region $\kappa_1^c < \kappa < \kappa_2^c$ of the intermediate phase.

INTRODUCTION. – Much theoretical progress has been made in the search for exotic states in frustrated two-dimensional (2D) quantum spin-lattice models that have no classical counterparts. A special role is reserved for the 2D triangular lattice, which is the simplest of the Archimedean lattices that exhibit geometric frustration (*i.e.*, which are not bipartite) and the one with the highest coordination number. For the triangular-lattice Heisenberg antiferromagnet (HAFM), comprising spins (with spin quantum number s) interacting via a pure nearest-neighbour (NN) Heisenberg potential with exchange coupling $J_1 > 0$, the classical ($s \to \infty$) ground state (GS) is a 3-sublattice Néel state with an angle of 120° between the spins on different sublattices, thereby breaking the translational symmetry of the lattice. When Anderson first introduced the concept of a resonating valence-bond (RVB) state [1, 2], it was hypothesized that the GS of the spin-$\frac{1}{2}$ HAFM on the triangular lattice with NN interactions only, could be such an RVB state, the first example of the quantum spin-liquid (QSL) states [3].

This conjecture was not supported by spin-wave theory (SWT), both at lowest (first) and second orders of implementation, which predict that the system retains the 3-sublattice 120° Néel antiferromagnetic (AFM) long-range (LRO), albeit with a reduction in the sublattice magnetization (*i.e.*, the magnetic order parameter) of about 50% for the $s = \frac{1}{2}$ case from the classical ($s \to \infty$) value [4–9]. Many other numerical studies, including variational calculations [10, 11], and some based on the exact diagonalization (ED) of small lattice clusters [12,13], lent credence to the SWT findings. A variety of recent high-accuracy numerical studies, including some based on the series expansion (SE) method [14], the ED method [15], the Green's function Monte Carlo (GFMC) method [16], the density-matrix renormalization group (DMRG) method [17], and the coupled cluster method (CCM) [18,19], all now concur that the GS of the spin-$\frac{1}{2}$ triangular-lattice HAFM with NN couplings only has the 3-sublattice 120° Néel ordering, with a sublattice magnetization in the rather accurately determined range of $(40 \pm 2)\%$ of the classical value.

To investigate a possible instability of the 120° Néel phase against the formation of more exotic GS phases, it is natural to add additional dynamic frustration by, for example, including an additional Heisenberg interaction between next-nearest-neighbour (NNN) pairs of spins with an exchange coupling $J_2 \equiv \kappa J_1$. The study of the resulting spin-$\frac{1}{2}$ J_1–J_2 model on the triangular lattice is the main aim of the present paper, particularly in the most interesting region of the parameters, $J_1 > 0$ and $0 \leq \kappa \leq 1$.

A number of recent studies [19–24] have shown the existence of a magnetically disordered quantum state in a range $\kappa_1^c < \kappa < \kappa_2^c$, beyond the range $\kappa < \kappa_1^c$ for which the 120° Néel ordering persists, and around the corresponding point $\kappa_1^{\rm cl} = \frac{1}{8}$ in the classical ($s \to \infty$) version of the model at which the 120° Néel order melts. Nevertheless, there remains disagreement over the values of the quantum critical points (QCPs) κ_1^c and κ_2^c, and also the nature of this intermediate phase. For example, a Schwinger boson mean-field theory (SBMFT) study [20] gives $\kappa_1^c \approx 0.12$ and $\kappa_2^c \approx 0.19$. By contrast, two different variational Monte Carlo (VMC) studies give $\kappa_1^c \approx 0.05$ and $\kappa_2^c \approx 0.18$ [21], and $\kappa_1^c \approx 0.10(1)$ and $\kappa_2^c \approx 0.135(5)$ [22]. Both VMC

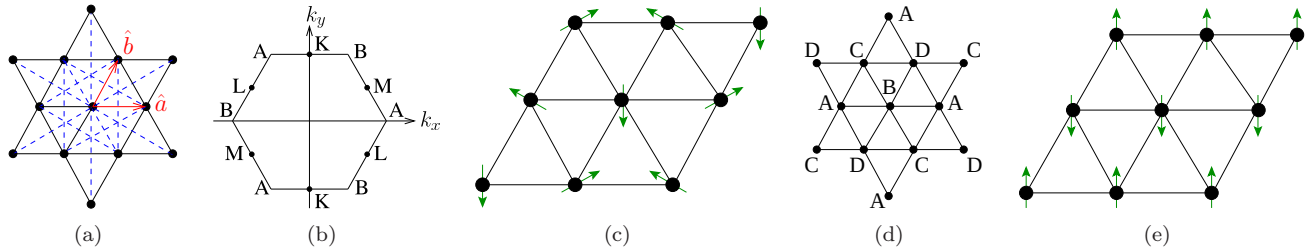

Fig. 1: (Colour on-line) The J_1–J_2 model on the triangular lattice, showing (a) the bonds ($J_1 \equiv$ —— ; $J_2 \equiv$ – – –) and the Bravais lattice vectors $\hat{a}$ and $\hat{b}$; (b) the corresponding first Brillouin zone; (c) the 120° Néel antiferromagnetic (AFM) state; (d) the infinitely degenerate family of classical 4-sublattice ground states on which the spins on the same sublattice are parallel to each other, with the sole constraint that the sum of four spins on different sublattices is zero; and (e) one of the three degenerate striped AFM states. For the two states shown the arrows represent the directions of the spins located on lattice sites •.

studies favour the intermediate state to be a gapless QSL, although of different types. However, both the SMBFT and VMC techniques involve either uncontrolled approximations and/or inbuilt bias towards certain forms of order.

Two essentially unbiased *ab initio* methods, with controlled approximations, that have been applied to the model are the CCM [19] and the DMRG [23–25]. Three recent studies give good agreement on the QCPs. The CCM study [19] gives $\kappa_1^c \approx 0.060(10)$ and $\kappa_2^c \approx 0.165(5)$, while two separate DMRG studies give $\kappa_1^c \approx 0.06$ and $\kappa_2^c \approx 0.17$ [23], and $\kappa_1^c \approx 0.08$ and $\kappa_2^c \approx 0.16$ [24]. (In the third recent DMRG study [25] the model was studied on a three-leg cylinder, for which no intermediate phase was found.) The two DMRG studies [23, 24] both favour the intermediate state to be a gapped QSL. Since the nature of the intermediate state has not yet been investigated within the CCM, which method probably provides the most accurate values available of the QCPs κ_1^c and κ_2^c, our primary aim here is to study it via its spin gap. Our main finding will be that, in sharp contrast to both recent DMRG studies [23, 24], the intermediate state is *gapless* over the entire regime $\kappa_1^c < \kappa < \kappa_2^c$, just as was found in the two earlier VMC studies [21, 22].

THE MODEL. – We study the Hamiltonian

$$H = J_1 \sum_{\langle i,j \rangle} \mathbf{s}_i \cdot \mathbf{s}_j + J_2 \sum_{\langle\langle i,k \rangle\rangle} \mathbf{s}_i \cdot \mathbf{s}_k \,, \qquad (1)$$

where $\langle i,j \rangle$ and $\langle\langle i,k \rangle\rangle$ run over NN and NNN pairs of sites, respectively, counting each bond once only. Each site i of the triangular lattice (with lattice spacing a) carries a spin-$\frac{1}{2}$ particle with spin operator $\mathbf{s}_i = (s_i^x, s_i^y, s_i^z)$. The lattice and the exchange bonds are illustrated in fig. 1(a). The first Brillouin zone for the triangular lattice is a hexagon of side $4\pi/3a$, as shown in fig. 1(b).

Classically, the spin configurations can be described by a wave vector $\mathbf{Q}$, such that the spin on site i is given by

$$\mathbf{s}_i = s[\cos(\mathbf{Q} \cdot \mathbf{r}_i)\hat{n}_1 + \sin(\mathbf{Q} \cdot \mathbf{r}_i)\hat{n}_2] \,, \qquad (2)$$

where $\hat{n}_1$ and $\hat{n}_2$ are two orthogonal unit vectors in spin space. In the regime $J_1 > 0$, and $0 \leq \kappa \leq 1$, where $\kappa \equiv J_2/J_1$, the corresponding classical ($s \to \infty$) phase diagram has just one phase transition at $\kappa_1^{\rm cl} = \frac{1}{8}$. For $\kappa < \kappa_1^{\rm cl}$ the system has the 3-sublattice 120° Néel ordering shown in fig. 1(c), described by either one of the two wave vectors representing the two inequivalent corners A and B of the first Brillouin zone shown in fig. 1(b), $\mathbf{Q}_A = \frac{4\pi}{a}(\frac{1}{3}, 0)$, $\mathbf{Q}_B = \frac{2\pi}{a}(\frac{1}{3}, \frac{1}{\sqrt{3}})$. For $1 > \kappa > \kappa_1^c$, the classical system has an infinitely degenerate family (IDF) of 4-sublattice Néel GS phases illustrated in fig. 1(d), in which the sole constraint is $\mathbf{s}_A + \mathbf{s}_B + \mathbf{s}_C + \mathbf{s}_D = 0$, where $\mathbf{s}_i$ denotes the spin on each of the four sublattices $i = A, B, C, D$, as shown. The application of lowest-order [*i.e.*, to $O(1/s)$] SWT has shown [26–28] that quantum fluctuations lift this accidental degeneracy in favour of the 2-sublattice striped states, one of which is shown in fig. 1(e), via the well-known order by disorder mechanism. These striped states have ferromagnetic ordering along one principal direction of the triangular lattice and AFM ordering along the other two principal directions. They are described by one of the three wave vectors representing the three inequivalent midpoints K, L, and M of the edges of the hexagonal first Brillouin zone shown in fig. 1(b), $\mathbf{Q}_K = \frac{2\pi}{a}(0, \frac{1}{\sqrt{3}})$, $\mathbf{Q}_L = \frac{\pi}{a}(-1, \frac{1}{\sqrt{3}})$, and $\mathbf{Q}_M = \frac{\pi}{a}(1, \frac{1}{\sqrt{3}})$.

In our present study we will use both classical GS phases, *viz.*, the 3-sublattice 120° Néel phase and the 2-sublattice striped state, as reference states, on top of which the quantum many-body correlations for the $s = \frac{1}{2}$ model will be systematically incorporated using the CCM.

THE COUPLED CLUSTER METHOD. – The CCM (see, *e.g.*, refs. [29–31]) is one of the most versatile, most accurate and most powerful techniques of *ab initio* quantum many-body theory. It has been applied to a huge variety of fields in physics and chemistry, including many strongly correlated and highly frustrated spin-lattice problems in quantum magnetism (see, *e.g.*, refs. [18,19,31–37]). Whereas many alternative methods require a finite-size scaling analysis, one of the main strengths of the CCM is that it is both size-consistent and size-extensive, and hence yields results from the outset in the 2D bulk ($N \to \infty$) limit. Another important feature is that it exactly pre-

serves the important Hellmann-Feynman theorem at *all* levels of approximate implementation. The method is utilized in practice at various levels of approximation, each specified by a truncation index $m = 1, 2, 3, \cdots$. The *only* approximation made in using of the CCM is then to extrapolate the sequences of values obtained for physical observables to the exact $m \to \infty$ limit.

Every implementation of the CCM starts with the choice of a suitable (normalized) reference (or model) state $|\Phi\rangle$, with respect to which the quantum corrections present in the exact GS $|\Psi\rangle$ may then be incorporated at the next step. Suitable choices for $|\Phi\rangle$ in the present case are the two quasiclassical AFM states [*viz.*, the 3-sublattice 120° Néel state of fig. 1(c) and the 2-sublattice striped state of fig. 1(e)]. The exact ket and bra GS wave functions $|\Psi\rangle$ and $\langle\tilde{\Psi}|$, which solve the respective Schrödinger equations $H|\Psi\rangle = E|\Psi\rangle$ and $\langle\tilde{\Psi}|H = E\langle\tilde{\Psi}|$, are chosen to have normalizations such that $\langle\tilde{\Psi}|\Psi\rangle = \langle\Phi|\Psi\rangle = \langle\Phi|\Phi\rangle = 1$. In terms of the chosen model state the CCM now utilizes its distinct exponential parametrizations, $|\Psi\rangle = e^S|\Phi\rangle$ and $\langle\tilde{\Psi}| = \langle\Phi|\tilde{S}e^{-S}$. The two GS correlation operators are themselves formally decomposed as $S = \sum_{I\neq 0} \mathcal{S}_I C_I^+$ and $\tilde{S} = 1 + \sum_{I\neq 0} \tilde{\mathcal{S}}_I C_I^-$, where we define $C_0^+ \equiv 1$ to be the identity operator, and where the set index I denotes a complete set of single-particle configurations for all of the N particles (*i.e.*, in our case, spins).

For spin-lattice applications each set index I represents a unique multispin-flip configuration with respect to $|\Phi\rangle$, such that the corresponding wave function for this configuration of spins is $C_I^+|\Phi\rangle$. We thus require $|\Phi\rangle$ to be chosen as a fiducial (or cyclic) vector (*i.e.*, in physical terms, a generalized vacuum state) with respect to the complete set of mutually commuting many-body creation operators $\{C_I^+\}$. In other words, we require C_I^+ and its destruction counterpart, $C_I^- \equiv (C_I^+)^\dagger$, to satisfy the conditions $\langle\Phi|C_I^+ = 0 = C_I^-|\Phi\rangle$, $\forall I \neq 0$.

It is useful to treat each lattice site i as equivalent to all others, whatever the choice of $|\Phi\rangle$. To that end we passively rotate each spin $\mathbf{s}_i$ so that in its own local spin-coordinate frame it points in the downward (*i.e.*, negative z_s) direction. Henceforth our description of the spins is given in terms of these locally defined spin-coordinate frames, in which all independent-spin product model states take the universal form $|\Phi\rangle = |\downarrow\downarrow\downarrow\cdots\downarrow\rangle$. Similarly, C_I^+ may be written in the universal form $C_I^+ \equiv s_{k_1}^+ s_{k_2}^+ \cdots s_{k_n}^+$; $n = 1, 2, \cdots, 2sN$, as a product of single-spin raising operators, $s_k^+ \equiv s_k^x + i s_k^y$. The set index $I \equiv \{k_1, k_2, \cdots k_n; n = 1, 2, \cdots, 2sN\}$ thus becomes a set of (possibly repeated) lattice site indices. For the present case, with $s = \frac{1}{2}$, each site index included in set index I may appear no more than once. Once the local spin coordinates have been chosen for a given $|\Phi\rangle$, the Hamiltonian H needs to be re-expressed in terms of them.

The GS CCM c-number correlation coefficients $\{\mathcal{S}_I, \tilde{\mathcal{S}}_I\}$ are now calculated by requiring that the GS energy expectation functional, $\bar{H} = \bar{H}[\mathcal{S}_I, \tilde{\mathcal{S}}_I] \equiv \langle\Phi|\tilde{S}e^{-S}He^S|\Phi\rangle$, be minimized with respect to each of them separately. This yields the coupled set of nonlinear equations $\langle\Phi|C_I^- e^{-S}He^S|\Phi\rangle = 0$; $\forall I \neq 0$, for the coefficients $\{\mathcal{S}_I\}$, and the coupled set of linear generalized eigenvalue equations $\langle\Phi|\tilde{S}[e^{-S}He^S, C_I^+]|\Phi\rangle = 0$; or equivalently, $\langle\Phi|\tilde{S}(e^{-S}He^S - E)C_I^+|\Phi\rangle = 0$, $\forall I \neq 0$, for the coefficients $\{\tilde{\mathcal{S}}_I\}$, once the coefficients $\{\mathcal{S}_I\}$ are solved for. Having solved for $\{\mathcal{S}_I, \tilde{\mathcal{S}}_I\}$, one may then, for example, calculate all GS properties such as the energy $E = \langle\Phi|e^{-S}He^S|\Phi\rangle$ and the magnetic order parameter (*i.e.*, the average local on-site magnetization) $M \equiv -\frac{1}{N}\langle\Phi|\tilde{S}\sum_{k=1}^N e^{-S}s_k^z e^S|\Phi\rangle$.

Excited-state (ES) wave functions are parametrized within the CCM as $|\Psi_e\rangle = X^e e^S|\Phi\rangle$, in terms of a linear excitation operator $X^e = \sum_{I\neq 0} \mathcal{X}_I^e C_I^+$. By combining the GS Schrödinger equation with its ES counterpart, $H|\Psi_e\rangle = E_e|\Psi_e\rangle$, and using that $[X^e, S] = 0$, we find $e^{-S}[H, X^e]e^S|\Phi\rangle = \Delta_e X^e|\Phi\rangle$, where $\Delta_e \equiv (E_e - E)$ is the excitation energy. By taking the overlap with the state $\langle\Phi|C_I^-$ we find $\langle\Phi|C_I^-[e^{-S}He^S, X^e]|\Phi\rangle = \Delta_e\mathcal{X}^e|\Phi\rangle$; $\forall I \neq 0$, where we have used that the states labelled by the set indices I are orthonormalized, $\langle\Phi|C_I^- C_J^+|\Phi\rangle = \delta(I, J)$. These generalized eigenvalue equations may then be solved for the set $\{\mathcal{X}_I^e\}$ and Δ.

No approximations have yet been made. One might expect that truncations are needed in the evaluation of the exponential functions $e^{\pm S}$ in the CCM parametrizations. However, we note that these always appear only in the form of the similarity transform $e^{-S}He^S$ of the Hamiltonian in all of the GS or ES equations we need to solve. This similarity transform may be expanded in terms of the well-known nested commutator series. Another key feature of the CCM is that this otherwise infinite series actually now terminates exactly at the double commutator term. This is due to the basic SU(2) commutation relations and the fact that all of the terms in the expansion $\sum_{I\neq 0} \mathcal{S}_I C_I^+$ for S commute with one another and are simple products of single-spin raising operators. Furthermore, all terms in the expansion for $e^{-S}He^S$ are thus linked. Hence, the Goldstone linked cluster theorem and the consequent size-extensivity of the method are exactly preserved even if the expansion for S is truncated.

Thus, the *only* approximation made in practical implementations of the CCM is to restrict the set of indices $\{I\}$ retained in the corresponding expansions for the operators $\{S, \tilde{S}\}$. As in our previous work on this model [19], and in many other applications of the CCM to quantum magnets, we use here the well-tested localized (lattice-animal-based subsystem) LSUBm scheme. At the mth level of approximation all multispin-flip configurations $\{I\}$ are retained in the expansions for S and $\tilde{S}$ that are constrained to no more than m contiguous sites. A cluster configuration is contiguous if every site in it is NN to at least one other. By utilizing the space- and point-group symmetries of the model, together with any conservation laws that apply to both the Hamiltonian and the model state under study, we may reduce the terms retained to a min-

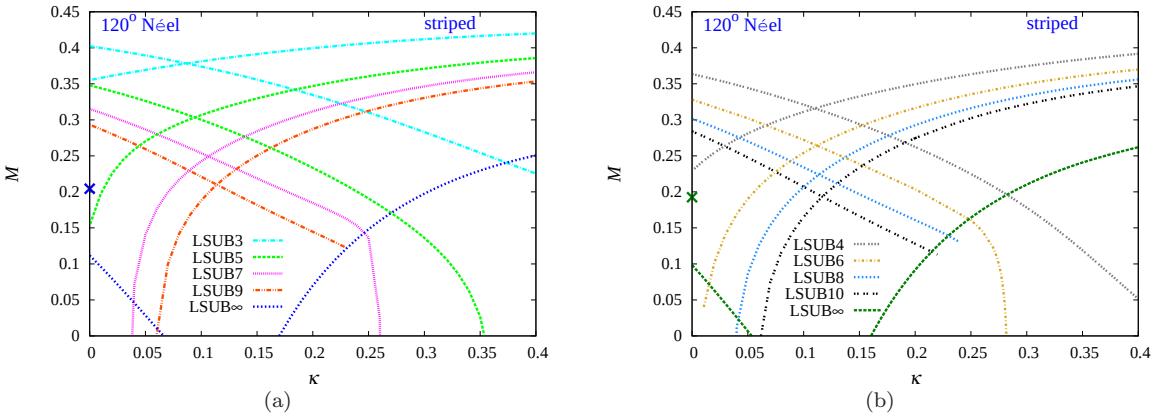

Fig. 2: (Colour on-line) CCM results for the GS magnetic order parameter M versus the frustration parameter $\kappa \equiv J_2/J_1$, for the spin-$\frac{1}{2}$ J_1–J_2 model on the triangular lattice (with $J_1 > 0$). The left and right sets of curves in each panel are based on the 120° Néel and striped AFM states, respectively, as CCM model states. The LSUBm results are shown: (a) with $m = \{3, 5, 7, 9\}$; and (b) with $m = \{4, 6, 8, 10\}$. In both cases the extrapolated LSUB∞ results using the respective data set in eq. (4) are shown. We also show with cross ($\times$) symbols the corresponding extrapolated values based on the 120° Néel state using eq. (3) for the case $\kappa = 0$ (*i.e.*, the pure triangular-lattice HAFM with NN interactions only).

imal number $N_f = N_f(m)$ of fundamental LSUBm configurations. Nevertheless, $N_f(m)$ increases rapidly as the truncation index m is increased, and one soon needs to use massive parallelization and supercomputing resources for the higher-order calculations [32,38].

For the ES calculation of the (magnon, triplet) spin gap Δ the choice of cluster configuration $\{I\}$ retained in the expansion for the excitation operator X^e is different from those for the GS correlation operators S and $\tilde{S}$, and different too for each model state, since we now restrict attention to those that change the z component of total spin, S^z, by one unit (in the local spin-coordinate frames), rather than to those with $S^z = 0$ for the GS calculation. However, to ensure comparable accuracy for both the GS and ES calculations, we use the LSUBm scheme in each case. The number $N_f(m)$, for a given value of m, is appreciably higher for the ES case than for the corresponding GS case using the same model state. The corresponding GS CCM LSUBm equations have been solved for both model states for $m \leq 10$. Whereas we can also solve the ES LSUBm equations for $m \leq 10$ for the striped state, the number $N_f(10)$ for the ES using the 120° Néel state is now sufficiently large that we are restricted in practice to $m \leq 9$ in this case.

Clearly, the CCM LSUBm approximations become exact, by construction, in the $m \to \infty$ limit. Thus, although the CCM obviates the need for any finite-size scaling, we do need to extrapolate our LSUBm results to the $m \to \infty$ limit as our last step and as our sole approximation. There exist very well-tested accurate extrapolation rules for such GS quantities as the energy per spin, E/N, and the magnetic order parameter, M, as we have described and used in our previous paper [19] on this model. For example, as we discussed there, for unfrustrated models or ones with relatively minor amounts of frustration we use

$$M(m) = b_0 + b_1 m^{-1} + b_2 m^{-2}\,, \tag{3}$$

whereas for highly frustrated systems, especially ones close to a QCP, we use

$$M(m) = b_0 + b_1 m^{-1/2} + b_2 m^{-3/2}\,. \tag{4}$$

For the spin gap we use the extrapolation scheme [33,39]

$$\Delta(m) = d_0 + d_1 m^{-1} + d_2 m^{-2}\,. \tag{5}$$

Of course, for the GS expectation value of any parameter P, we may always fit our LSUBm data to an asymptotic form $P(m) = p_0 + p_1 m^{-\nu}$, in order to extract the leading exponent ν. For our $\Delta(m)$ results, for example, we find $\nu \approx 1$ for all values of κ, which hence justifies the use of Eq. (5). Whenever possible we fit each of the extrapolation schemes of eqs. (3)–(5), all of which contain three fitting parameters, to LSUBm results with at least four different values of m. Since the triangle is the basic structural element of the lattice, the lowest-order results with $m < 3$ are excluded from the extrapolations.

RESULTS. – We show in fig. 2 our results for the magnetic order parameter M for the model, using both the 120° Néel and striped AFM states as CCM model states. Since the LSUBm results show a marked even-odd staggering effect in the truncation index m, we display the odd and even values separately in figs. 2(a) and 2(b), together with the associated LSUB∞ extrapolations using eq. (4), which is appropriate in the highly frustrated regions near the QCPs, together with the value using eq. (3) for the unfrustrated case $\kappa = 0$ only. The QCPs (*viz.*, the points κ at which the extrapolated LSUB∞ values for

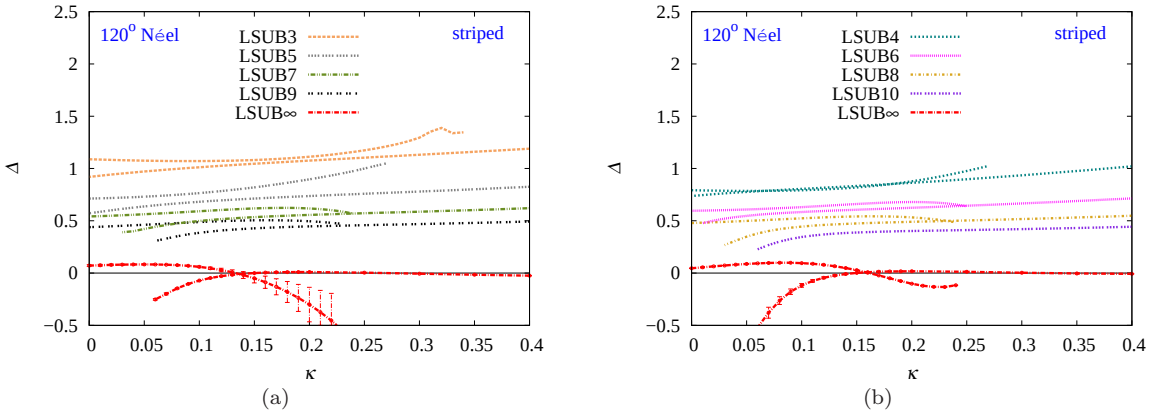

Fig. 3: (Colour on-line) CCM results for the spin gap Δ versus the frustration parameter $\kappa \equiv J_2/J_1$, for the spin-$\frac{1}{2}$ J_1–J_2 model on the triangular lattice (with $J_1 = 1$). The left and right sets of curves in each panel are based on the 120° Néel and striped AFM states, respectively, as CCM model states. The LSUBm results are shown: (a) with $m = \{3, 5, 7, 9\}$; and (b) with $m = \{4, 6, 8\}$ for the 120° Néel state and $m = \{4, 6, 8, 10\}$ for the striped state. In both cases the extrapolated LSUB∞ results using the respective data sets in eq. (5) are shown, together with error bars associated with the fits using four data points.

M vanish) show great consistency between those based on even m values and those based on odd m values. A careful analysis of our errors gives our best estimates for the two QCPs as $\kappa_1^c = 0.060 \pm 0.010$ and $\kappa_2^c = 0.165 \pm 0.005$. We note, parenthetically, that the smooth shape of the $M(\kappa)$ curves in fig. 2 near both QCPs lends support to both transitions being continuous. However, since the extrapolations near any critical point are very sensitive, we cannot entirely rule out the possibility of either transition being first-order.

An interesting feature of our LSUBm results displayed in fig. 2 is that we find solutions based on a given model state over a region that extends beyond the associated exact (LSUB∞) QCP, typically out to some associated termination point $\kappa^t(m)$, beyond which, at a given LSUBm level of approximation, no real solution exists. Such termination points have been found in many other applications and are very well understood. They have been shown [31] to be direct manifestations of the associated QCP (at κ^c, say) at which the order of the model state melts in the physical system. Typically the extent $|\kappa^t(m) - \kappa^c|$ of the region of unphysical intrusion of the solution with the order properties of the CCM model state into the neighbouring phase (beyond the QCP at κ^c) in which this form of order vanishes, decreases as the truncation index m is increased, and vanishes in the exact limit $m \to \infty$. It is clear from fig. 2 that these regions of unphysical intrusion of the CCM LSUBm solutions into the regime $\kappa_1^c < \kappa < \kappa_2^c$ of the intermediate phase cover essentially the whole intermediate region for all values $m \leq 10$ on both the neighbouring 120° Néel and striped quasiclassical AFM sides. For that reason we are now well placed to investigate the intermediate phase regime using both quasiclassical model states.

Thus, in figs. 3(a) and 3(b) we show our corresponding LSUBm results for the spin gap Δ, together with the extrapolated LSUB∞ values using eq. (5). Goldstone's theorem implies that any state breaking spin-rotational symmetry, including all states with magnetic LRO, must have a vanishing gap. We see from figs. 3(a) and 3(b) that our extrapolated LSUB∞ results for Δ are wholly consistent with $\Delta = 0$ for the striped state, $\kappa > \kappa_2^c \approx 0.165$. The results on the (computationally more challenging) 120° Néel-ordered side, $\kappa < \kappa_1^c \approx 0.06$, are slightly less accurate, but still compatible with Goldstone's theorem, within small errors, presumably associated with extrapolations in this region being less accurate.

Most interestingly, the results in fig. 3 based on both quasiclassical AFM states show no tendency at all for the spin gap Δ to increase in the regions of the intermediate phase accessible by the unphysical intrusion effect. Of course, the spin gap, by definition, satisfies $\Delta \geq 0$. The regions where $\Delta < 0$ in fig. 3 are clearly wholly unphysical therefore. However, our results are invalid in the regions beyond where the curves based on each model state cross, since the value of Δ is, by definition, unique. Beyond the crossing point we are simply too far into the unphysical regime, and we see from fig. 3 that this is reflected in the large error bars there. We note too that our largest error for Δ on the 120° Néel ordered side (where $\Delta = 0$ is exact) is $\Delta \lesssim 0.1$, which is compatible with the values we obtain for Δ in the intermediate regime. The extrapolated values of the spin gap are thus compatible with the spin gap vanishing essentially everywhere within the intermediate phase region, $\kappa_1^c < \kappa < \kappa_2^c$. For comparison, we note that the estimate obtained by a recent DMRG study [24] for the *bulk* triplet gap is $\Delta \approx 0.3 \pm 0.1$ at $\kappa = 0.1$, which is clearly at odds with our results.

SUMMARY AND DISCUSSION. – Our primary finding is that we find no evidence at all for any part of the intermediate phase to be a gapped state. We may compare our study with similar recent CCM spin-gap studies of both the spin-$\frac{1}{2}$ J_1–J_2 model on the square lattice [39] and the spin-$\frac{1}{2}$ J_1–J_2–J_3 model on the honeycomb lattice (with $J_3 = J_2$) [40]. For the former model Δ was again found to be zero over that part of the equivalent intermediate phase region accessible by the unphysical intrusion mechanism, which was not the whole region in this case. By contrast, for the latter model, strong evidence was found that $\Delta \neq 0$ over the similarly accessible part of its equivalent intermediate phase, which finding provides strong support for that phase having valence-bond crystalline (VBC) order, as is now broadly agreed.

Finally, in contrast to the recent DMRG studies [23, 24] that find the intermediate phase of the spin-$\frac{1}{2}$ J_1–J_2 model on the triangular lattice to be a gapped QSL, our CCM results indicate that the intermediate phase is gapless. While our results clearly preclude the intermediate phase in this model to have any form of VBC order, since any such state is gapped, they point towards a gapless QSL as the most likely candidate.

* * *

We thank the University of Minnesota Supercomputing Institute for the grant of supercomputing facilities. One of us (RFB) acknowledges the Leverhulme Trust for the award of an Emeritus Fellowship (EM-2015-07).

REFERENCES

[1] Anderson P. W., *Mater. Res. Bull.*, **8** (1973) 153.
[2] Fazekas P. and Anderson P. W., *Philos. Mag.*, **30** (1974) 423.
[3] Balents L., *Nature*, **464** (2010) 199.
[4] Oguchi T., *J. Phys. Soc. Jpn. Suppl.*, **52** (1983) 183.
[5] Nishimori H. and Miyake S. J., *Prog. Theor. Phys.*, **73** (1985) 18.
[6] Jolicoeur Th. and Le Guillou J. C., *Phys. Rev. B*, **40** (1989) 2727.
[7] Miyake S. J., *J. Phys. Soc. Jpn.*, **61** (1992) 983.
[8] Chubukov A. V., Sachdev S. and Senthil T., *J. Phys.: Condens. Matter*, **6** (1994) 8891.
[9] Chernyshev A. L. and Zhitomirsky M. E., *Phys. Rev. B*, **79** (2009) 144416.
[10] Huse D. A. and Elser V., *Phys. Rev. Lett.*, **60** (1988) 2531.
[11] Sindzingre P., Lecheminant P. and Lhuillier C., *Phys. Rev. B*, **50** (1994) 3108.
[12] Bernu B., Lhuillier C. and Pierre L., *Phys. Rev. Lett.*, **69** (1992) 2590.
[13] Bernu B., Lecheminant P., Lhuillier C. and Pierre L., *Phys. Rev. B*, **50** (1994) 10048.
[14] Zheng W., Fjærestad J. O., Singh R. R. P., McKenzie R. H. and Coldea R., *Phys. Rev. B*, **74** (2006) 224420.
[15] Richter J., Schulenburg J. and Honecker A., *Quantum magnetism in two dimensions: From semi-classical Néel order to magntic disorder* in *Quantum Magnetism*, edited by Schollwöck U., Richter J., Farnell D. J. J. and Bishop R. F., Lecture Notes in Physics Vol. 645 (Springer-Verlag, Berlin) 2004 pp. 85–153.
[16] Capriotti L., Trumper A. E. and Sorella S., *Phys. Rev. Lett.*, **82** (1999) 3899.
[17] White S. R. and Chernyshev A. L., *Phys. Rev. Lett.*, **99** (2007) 127004.
[18] Farnell D. J. J., Götze O., Richter J., Bishop R. F. and Li P. H. Y., *Phys. Rev. B*, **89** (2014) 184407.
[19] Li P. H. Y., Bishop R. F. and Campbell C. E., *Phys. Rev. B*, **91** (2015) 014426.
[20] Manuel L. O. and Ceccatto H. A., *Phys. Rev. B*, **60** (1999) 9489.
[21] Mishmash R. V., Garrison J. R., Bieri S. and Xu C., *Phys. Rev. Lett.*, **111** (2013) 157203.
[22] Kaneko R., Morita S. and Imada M., *J. Phys. Soc. Jpn.*, **83** (2014) 093707.
[23] Zhu Z. and White S. R., *Phys. Rev. B*, **92** (2015) 041105(R).
[24] Hu W.-J., Gong S.-S., Zhu W. and Sheng D. N., *Phys. Rev. B*, **92** (2015) 140403(R).
[25] Saadatmand S. N., Powell B. J. and McCulloch I. P., *Phys. Rev. B*, **91** (2015) 245119.
[26] Jolicoeur Th., Dagotto E., Gagliano E. and Bacci S., *Phys. Rev. B*, **42** (1990) 4800(R).
[27] Chubukov A. V. and Jolicoeur Th., *Phys. Rev. B*, **46** (1992) 11137.
[28] Korshunov S. E., *Phys. Rev. B*, **47** (1993) 6165.
[29] Bishop R. F., *Theor. Chim. Acta*, **80** (1991) 95.
[30] Bishop R. F., *The coupled cluster method* in *Microscopic Quantum Many-Body Theories and Their Applications*, edited by Navarro J. and Polls A., Lecture Notes in Physics Vol. 510 (Springer-Verlag, Berlin) 1998 p. 1.
[31] Farnell D. J. J. and Bishop R. F., *The coupled cluster method applied to quantum magnetism* in *Quantum Magnetism*, edited by Schollwöck U., Richter J., Farnell D. J. J. and Bishop R. F., Lecture Notes in Physics Vol. 645 (Springer-Verlag, Berlin) 2004 p. 307.
[32] Zeng C., Farnell D. J. J. and Bishop R. F., *J. Stat. Phys.*, **90** (1998) 327.
[33] Krüger S. E., Richter J., Schulenburg J., Farnell D. J. J. and Bishop R. F., *Phys. Rev. B*, **61** (2000) 14607.
[34] Krüger S. E., Darradi R., Richter J. and Farnell D. J. J., *Phys. Rev. B*, **73** (2006) 094404.
[35] Bishop R. F., Li P. H. Y., Darradi R. and Richter J., *Europhys. Lett.*, **83** (2008) 47004.
[36] Li P. H. Y., Bishop R. F., Campbell C. E., Farnell D. J. J., Götze O. and Richter J., *Phys. Rev. B*, **86** (2012) 214403.
[37] Bishop R. F., Li P. H. Y. and Campbell C. E., *Phys. Rev. B*, **89** (2014) 214413.
[38] We use the program package CCCM of D. J. J. Farnell and J. Schulenburg, see http://www-e.uni-magdeburg.de/jschulen/ccm/index.html.
[39] Richter J., Zinke R. and Farnell D. J. J., *Eur. Phys. J. B*, **88** (2015) 2.
[40] Bishop R. F., Li P. H. Y., Götze O., Richter J. and Campbell C. E., *Frustrated Heisenberg antiferromagnet*

on the honeycomb lattice: Spin gap and low-energy parameters arXiv:1504.02275 (2015).